Journal of Coastal Research	15	1	74–86	Royal Palm Beach, Florida	Winter 1999

Sand Re-Suspension Events in a High Energy Infragravity Swash Zone

Philip D. Osborne and Geraldine A. Rooker

Department of Geography and
School of Environmental & Marine Sciences
Tamaki Campus
University of Auckland
Private Bag 92019
Auckland, New Zealand
E-mail: p.osborné@auckland.ac.nz

ABSTRACT

OSBORNE, P.D. and ROOKER, G.A., 1999. Sand re-suspension events in a high energy infragravity swash zone. *Journal of Coastal Research,* 15(1), 74–86. Royal Palm Beach (Florida), ISSN 0749-0208.

Suspended sediment concentration (SSC), fluid velocity and morphological response were measured on the foreshore of a high energy dissipative beach west of Auckland, New Zealand. Swash re-suspension events exhibit a distinct temporal structure associated with both the uprush and backwash phases. SSC of >50 gl $^{-1}$ is associated with large accelerations, turbulence, and high flow speeds in shallow water under shoreward propagating swash bores. SSC decreases rapidly from the initial peak and then more gradually as water depth increases to a maximum at the end of the uprush. SSC increases gradually as the backwash accelerates, and then reaches a peak under the rapidly thinning and accelerating flow near the end of the backwash. Flows are super-critical, hydraulic jumps occur and unstable anti-dune bedforms often develop near the end of backwash events resulting in sharp increases in SSC. Event averaged SSC declines systematically as maximum depth of swash increases. Peak SSC tends to be larger under uprush events than backwash events particularly near the margins of the swash zone. Cross-spectral analysis of velocity and SSC at the transition between the inner surf zone and swash zone confirms that the dominant transport occurs at infragravity frequencies. Net transport is potentially sensitive to small variations in the phase angle between SSC and velocity in the uprush and backwash cycle as well as to the variability in bed conditions during swash cycles.

Additional Index Words: *Sand transport, suspension events, high energy beach, infragravity, swash.*

INTRODUCTION

Observations of sand transport on beaches indicate that episodic suspension events occur in response to a variety of mechanisms, including long period infragravity and far-infragravity waves (BEACH and STERNBERG, 1992; AAGAARD and GREENWOOD, 1994), short period waves and wave groups (HANES, 1991; DICK *et al.*, 1994). The causes of episodicity and the relative importance of various hydrodynamic mechanisms in producing net sediment transport are not fully understood. Studies of sediment suspension and transport in the nearshore have been focussed on the surf zone and shoreface; the latter is dominated by relatively short period incident waves. In contrast, there are few observations of suspended sand concentrations from the swash zone (see review by HORN and MASON, 1994) and only one published set of measurements using fast response sensors. BEACH and STERNBERG (1991) and HORN and MASON (1994) have reported that concentrations of suspended sand are several times larger in the swash zone than in the surf zone and offshore regions. Fast response measurements by BEACH and STERNBERG (1991) indicate that swash zone sediment transport is dominated by infragravity waves. Considering the large quantities of suspended sand in the swash zone and the overall importance of swash processes to beach erosion and accretion, it is likely that the relative timing and magnitude of suspension events is important to the direction and magnitude of net cross-shore transport in the swash zone. So far there has been no systematic examination of the spatial and temporal structure of suspension events in the swash zone.

In this paper we describe field measurements of the of near bed fluid velocity (U, V, W), water surface elevations (η) and suspended sand concentrations (SSC) obtained in the swash zone of a high energy dissipative beach. The objective is to examine the temporal structure of swash zone suspension events in relation to the local hydrodynamics in order to gain an improved understanding of the controls on net sediment transport and morphological response in this region.

Study Site and Measurements

The data described in this paper were obtained at Bethells Beach (Te Henga) which is situated on the west coast of the North Island of New Zealand (Figure 1). Bethells Beach is typical of the relatively undisturbed west coast beaches which are exposed to almost continuous high energy swell originating mainly from the southwest particularly in winter and spring (HESSELL, 1988). The meso-macro tidal regime (approximately 3.5 m at spring tides) with a relatively broad inter-tidal region (~100 m) allows instrumentation to be de-

97044 received 20 March 1997; accepted in revision 5 October 1997.

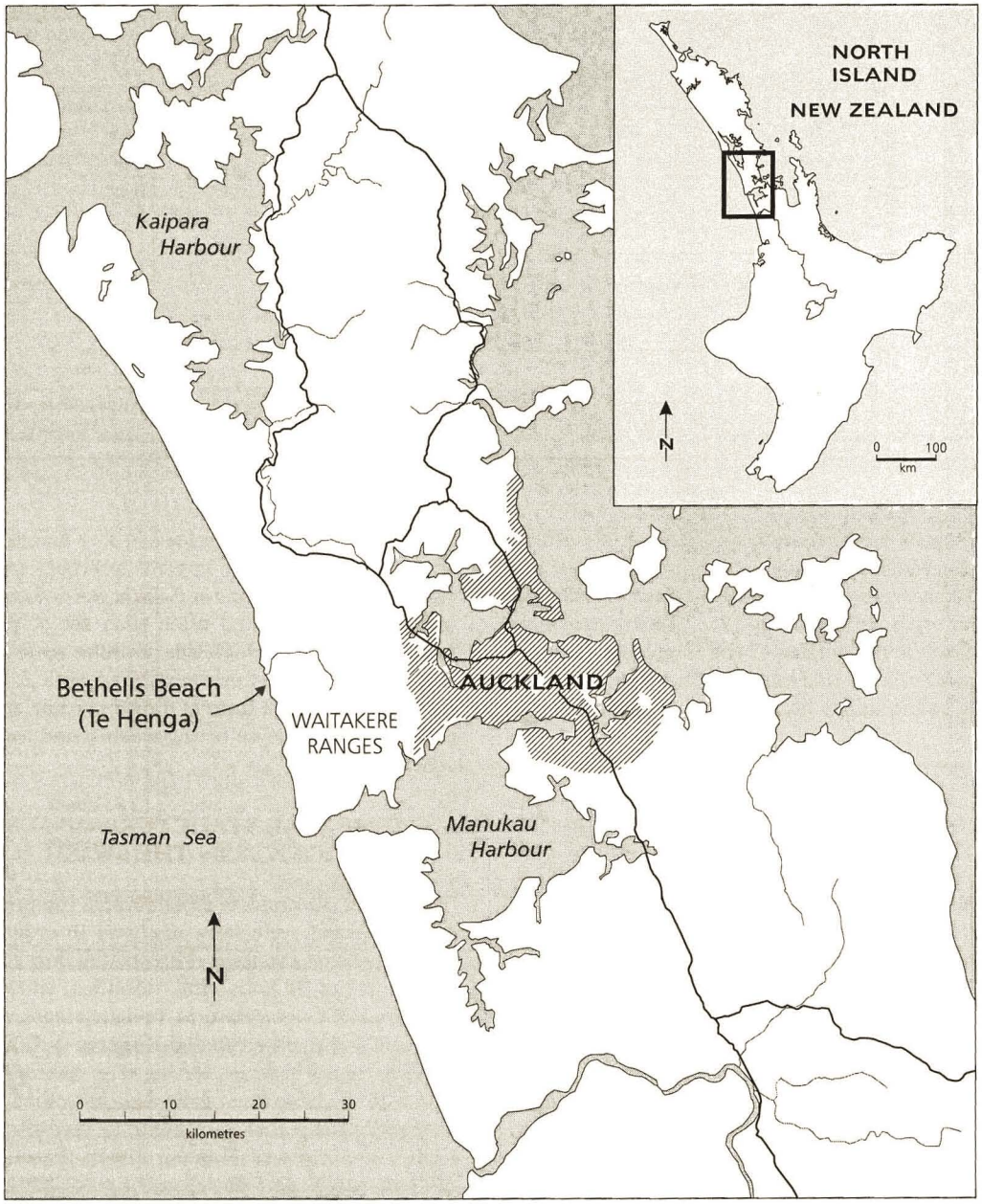

Figure 1. Location of study site.

ployed and recovered safely at low tide while process measurements can be obtained at high tide. The dissipative nature of the surf zone (width 200–400 m) prevents extreme offshore surf (common breaker heights of 2–5 m) from directly affecting the foreshore with the potential of destroying the instrumentation. The wide swash zone (30–60 m), dominated by cross-shore infragravity motions, allows frequent observations of bed elevation relative to sensors and observations of foreshore response between major swash events.

The beach is composed of the dense black "ironsands" which are common on the west coast of New Zealand's North Island. The "ironsand" consists mainly of titanomagnetite (15–40%), ilmenite (17%) and other heavy minerals plus small quantities of quartz and feldspars (HAYWARD, 1983). The sand in the vicinity of the instrumentation was well sorted fine-medium sand (2.7 ϕ, 0.150 mm) with a standard deviation of 0.26 ϕ. There were no apparent variations in sand size or mineralogy across the foreshore slope.

The experiments were conducted over four days in May and July, 1995, the measurements being taken over four high tide cycles with moderate to high energy incident swell present. Results presented here focus on the measurements taken on

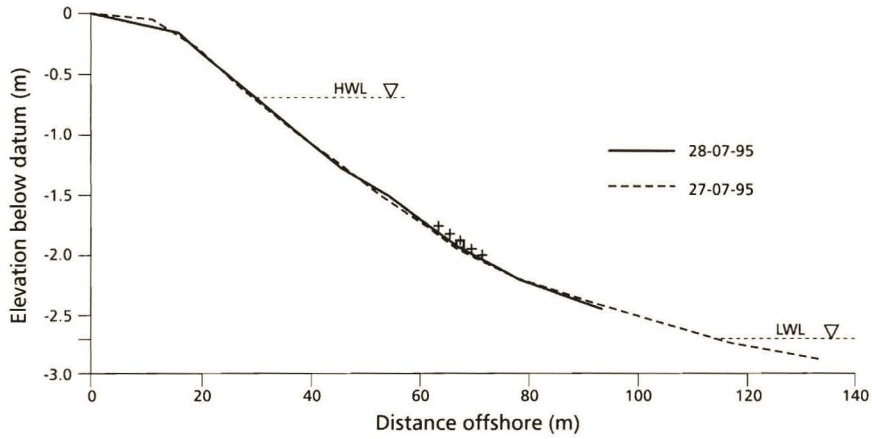

Figure 2. Beach profile showing location of instrumented station, depth-of-disturbance rods, and position of high and low water for 28-07-95.

July 28, 1995 when 23 time-series were collected. No direct measurements of the incident swell were obtained; swell reports and visual observations estimated incident significant heights of 1.5–2 m with periods of 10–12 s. The instruments were situated on the lower portion of the foreshore in order to be fully immersed at high tide and to be in the swash zone for up to 2 hours before and 2 hours after high tide (Figure 2).

Point measurements of 3-dimensional velocities in close proximity (within 2–5 cm) of the fluid-sediment boundary were obtained with a Sontek acoustic-Doppler velocimeter (ADV, LOHRMANN *et al.*, 1994). Measurements of near bed SSC were made using 2 optical backscatter sensors (OBS-3 by D&A Instruments). Water surface elevations were measured with a 1.5 m teflon coated capacitance wave gauge (WG-1 by Richard Brancker Research, Ltd.). The instruments were mounted with adjustable brackets on a 1.5 m^3 frame which was held in place with 4 guy wires attached to galvanised anchors (Figure 3). Sensors were collocated and aligned in the longshore direction with a horizontal (alongshore) separation of 30 cm. The ADV was set to measure currents at a nominal elevation of 5 cm above the bed and was vertically collocated with the lowermost OBS. A second OBS was situated 5 cm above the lower sensor. As the bed elevation changed over relatively short time scales it was necessary to measure and record sensor position before and after each burst of data collection. The vertical position of the sensors was adjusted frequently between bursts to maintain a consistent elevation for measurements.

The sensors were hardwired (100 m cable) to a shore-based power supply and a high speed data acquisition system controlled by laptop computer. Bursts of 4,100 data points were acquired at rates of 5, 10 and 20 Hz (record lengths of 805 s, 410 s and 205 s). The ADV data were calibrated using manufacturer supplied software and vertical velocities were corrected for small errors in the alignment of the probe. The OBS sensors and wave gauges were calibrated according to standard laboratory procedures for these instruments (*e.g.* OSBORNE *et al.*, 1994).

Beach morphological response was monitored at 2 spatial and temporal scales. Complete foreshore profiles were surveyed at low tide using a Sokkia Set-5 total station survey instrument before and after each set of process measurements was taken at high tide. Smaller scale changes (1–2 m^2) in beach response were monitored with a grid of depth of disturbance rods (3 lines of 6 rods per line spaced 1 m apart) equipped with a loose fitting washer and located around the sensor frame.

TEMPORAL STRUCTURE OF SUSPENSION EVENTS IN THE SWASH ZONE

A total of 54 complete swash events comprised of an uprush and backwash cycle were analysed in order to characterise the suspension events and associated flow conditions.

Time-series of horizontal velocities, water surface elevations and SSC measured at various stages of the tide on 28 July 1995 are illustrated in Figures 4–7. Segments of the velocity record in which the signal-noise ratio (SNR) dropped below 25 dB have been excluded (note that this is a conservative SNR threshold according to manufacturers specifications, Sontek Users Manual, 1994); these segments of low SNR represent periods when the velocimeter probe was out of the water. The first two series (Figures 4 and 5) are typical of time series at approximately the mid-point of rising and falling tides when the sensors were immersed intermittently in the swash zone under infragravity events while the series in Figure 6 represents the transition region between the swash zone and inner surf zone where the sensors were almost continuously immersed.

Long period cross-shore swash excursions (Figures 4–7e) dominate the velocity field and are characterised by large onshore-offshore motions with maximum speeds in either direction reaching 200 cm s^{-1} and with periods of approximately 50 s. A zero crossing analysis of time series when sensors were close to being continuously immersed (Figure 6e) at high tide indicates the significant onshore velocities were 145 cm s^{-1}. Smaller waves with periods of 12–15 s were super-

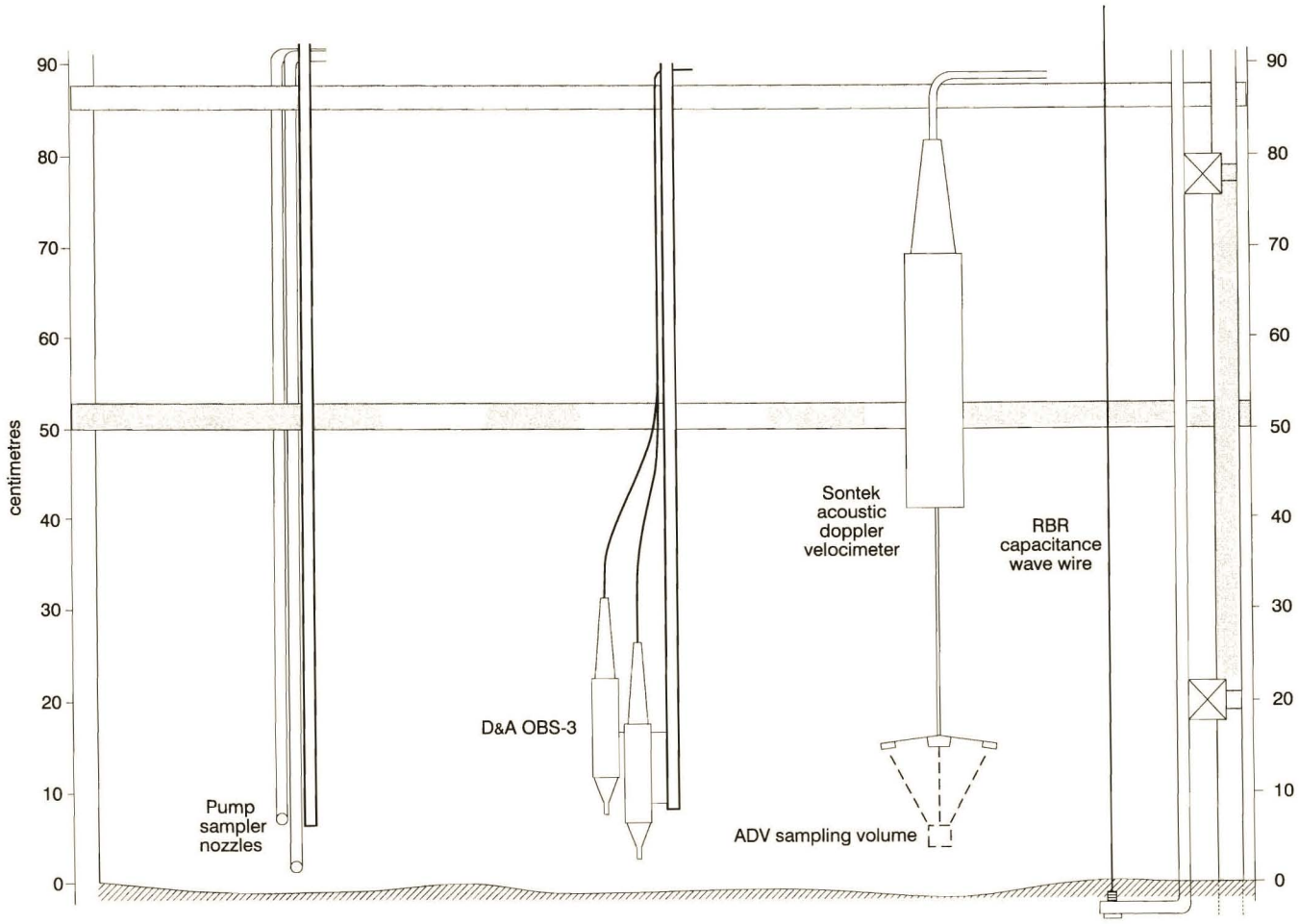

Figure 3. Schematic of instrumented station. Note: the horizontal scale is the same as the vertical scale.

imposed on this larger scale motion. Shore-parallel velocities were considerably weaker than cross-shore velocities with a range of 25 cm s^{-1} and mean speeds of 5–10 cm s^{-1} towards the north end of the beach. Instantaneous cross-shore current speeds were up to 8 times larger than instantaneous shore parallel velocities. Mean current speeds in the cross-shore direction were between 5–7 cm s^{-1} and directed offshore in the inner surf zone.

Figures 4–7c are time series of the turbulent kinetic energy (TKE) of the fluid which is equivalent to half the sum of the variances of the fluctuations in the three coordinate directions, times the density, ρ:

$$\frac{1}{2}\rho\overline{k^2} = \frac{1}{2}\rho(\overline{u'^2} + \overline{v'^2} + \overline{w'^2})$$

where u′, v′ and w′ are the turbulent fluctuations in the three coordinate directions (DYER, 1986). In this case, TKE is an estimate of the total velocity variance and not strictly the turbulent kinetic energy, as the flow kinematics are dominated by infragravity wave orbital motions which have been included in the estimates.

Concentrations (Figures 4–7a, b) develop and decay as discrete suspension events associated with the long period uprush and backwash events. The largest SSC occurs near the start and end of each event in association with high TKE. Instantaneous SSC may exceed 150 g l^{-1} while event averaged SSC ranged from 4–45 g l^{-1}. BEACH and STERNBERG (1992) have also reported peak SSC of similar magnitude in the swash zone of a high energy beach and measured average SSC up to 9 times larger than those found in the surf zone.

In order to examine the variation in SSC with variation in the position of instruments in the swash zone, SSC was averaged over the duration of each suspension event and then over all events in each burst to produce a burst-average SSC for each sensor elevation. This was completed for a total of 11 bursts of data preceding, during and following high tide when precise pre- and post-burst measurements of sensor elevation were available. Since sensor elevation varied from burst to burst it was necessary to predict SSC at a consistent reference elevation. In this instance, an arbitrary reference elevation of 2 cm above the boundary was chosen as the reference elevation. SSC at 2 cm was then predicted for each

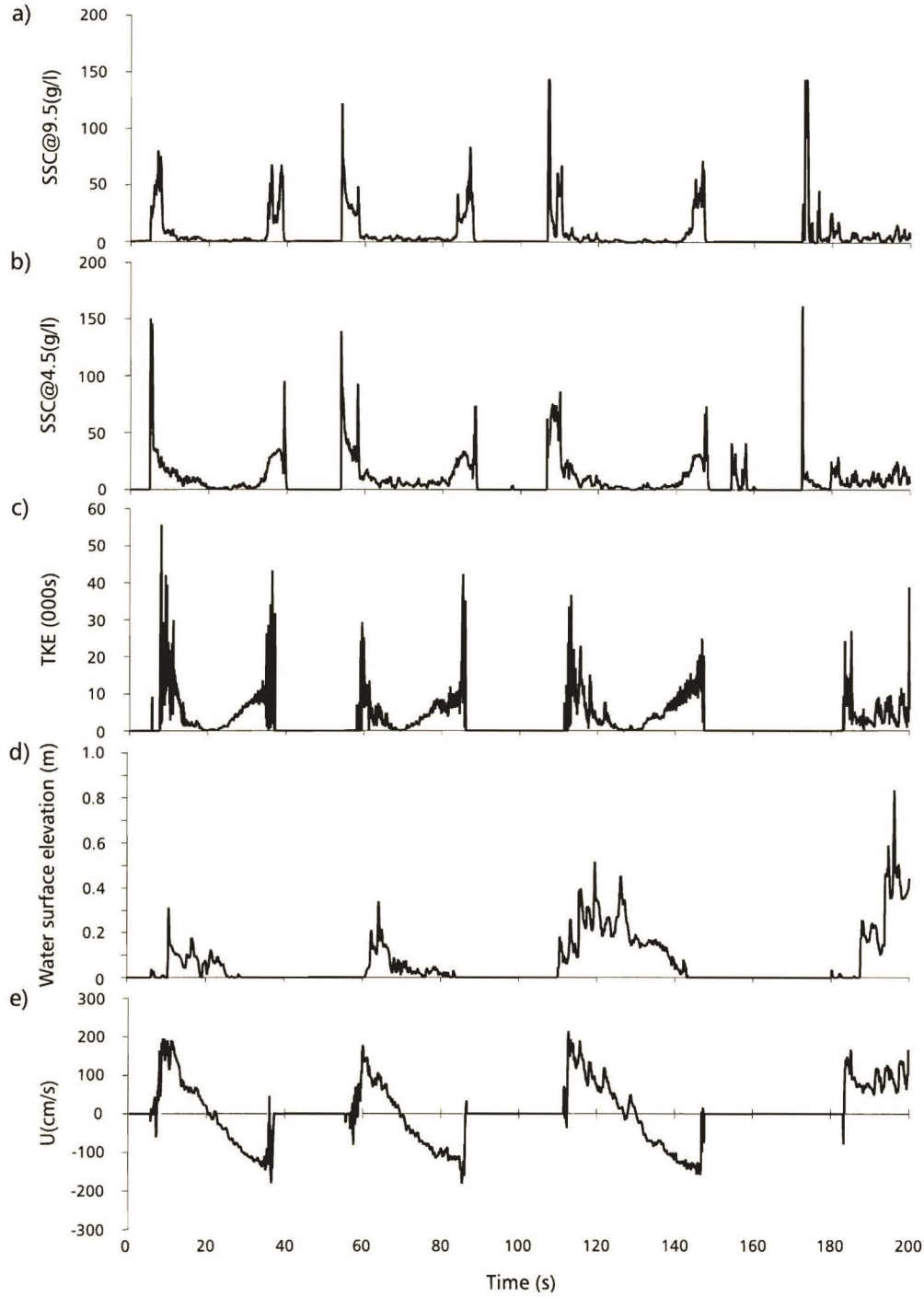

Figure 4. Time series of SSC at 9.5 cm and 4.5 cm elevation (a, b), turbulent kinetic energy (c), water surface elevation (d) and cross-shore velocity (e) from the mid swash zone on a rising tide (28-07-1995 8:24).

burst assuming an exponential SCC profile and a length scale (*e.g.* NEILSEN, 1984) for each burst determined from the gradient in SSC between the upper and lower sensor elevations. As water levels changed relative to the instrumented station under the rising and falling tide there was a corresponding decrease and increase in burst-averaged SSC at 2 cm (Figure 8). This inverse relationship between SSC and water depth suggests that much higher bed shear stresses are generated by the rapidly accelerating flows and turbulence at the start and end of the uprush and backwash when the water depth

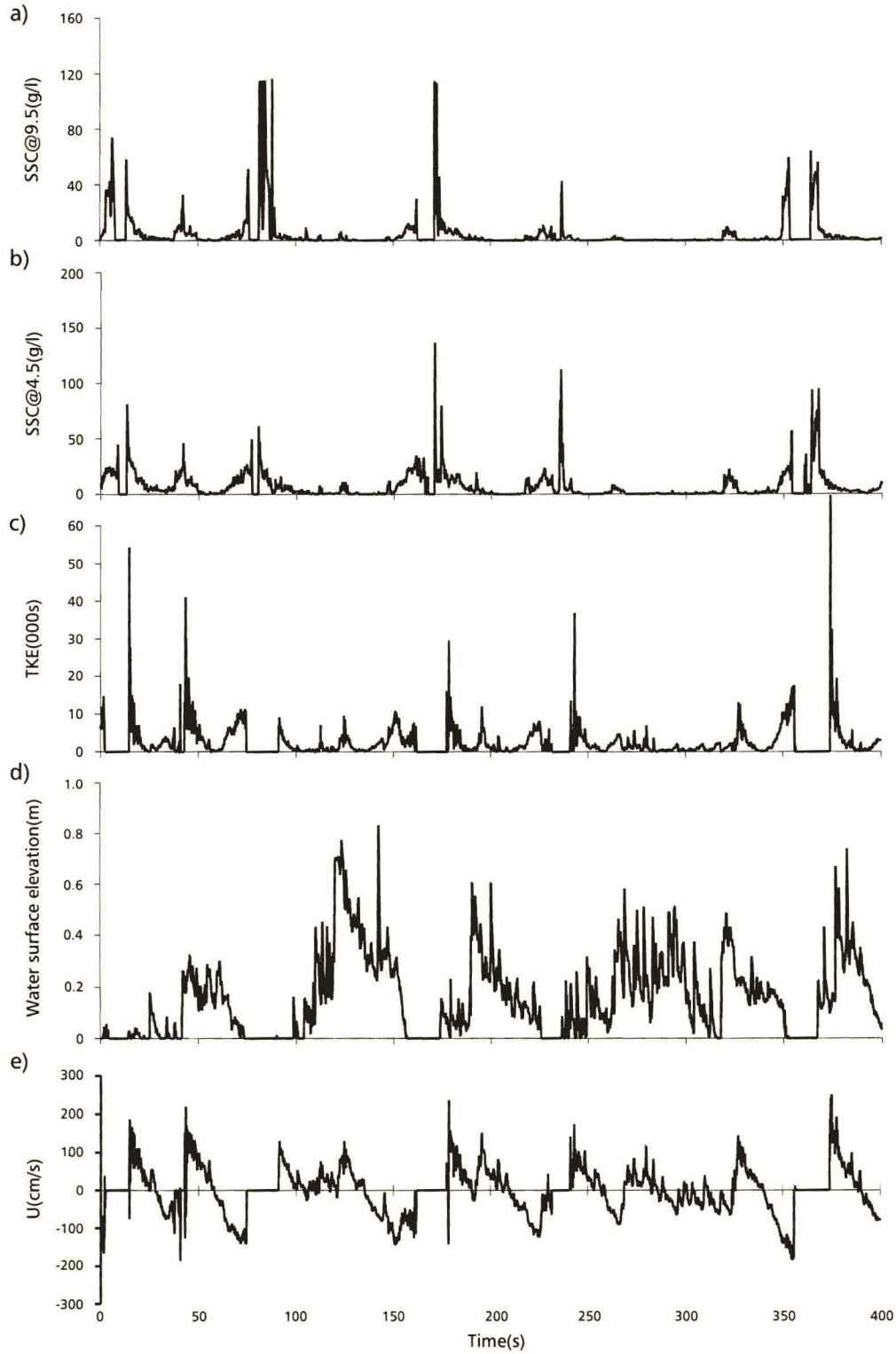

Figure 5. Time series of SSC at 9.5 cm and 4.5 cm elevation (a, b), turbulent kinetic energy (c), water surface elevation (d) and cross-shore velocity (e) from the mid swash zone on a rising tide (28-07-1995 8:45).

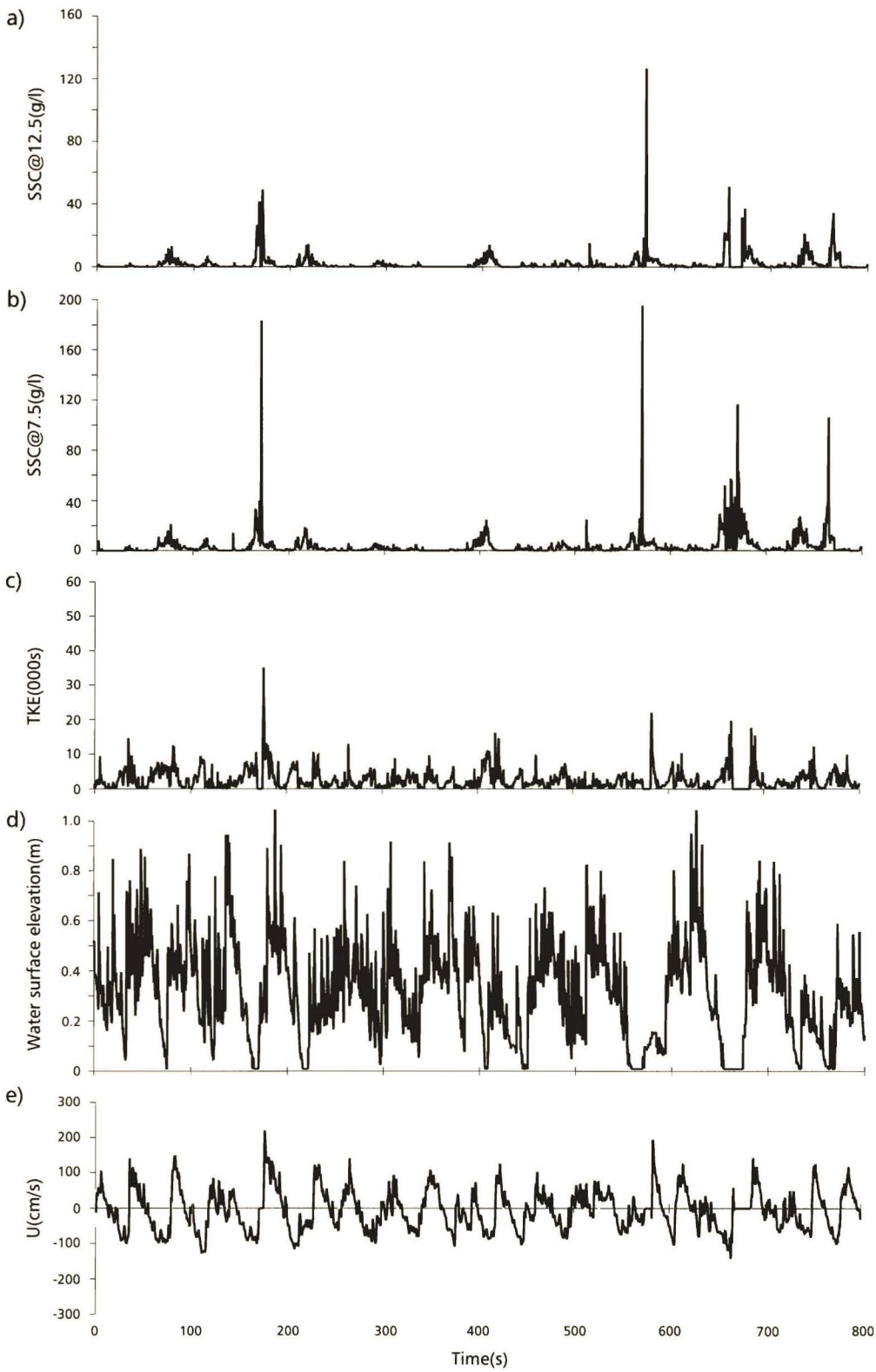

Figure 6. Time series of SSC at 12.5 cm and 7.5 cm elevation (a, b), turbulent kinetic energy (c), water surface elevation (d) and cross-shore velocity (e) from the swash zone-inner surf zone transition near high tide (28-07-1995 10:30).

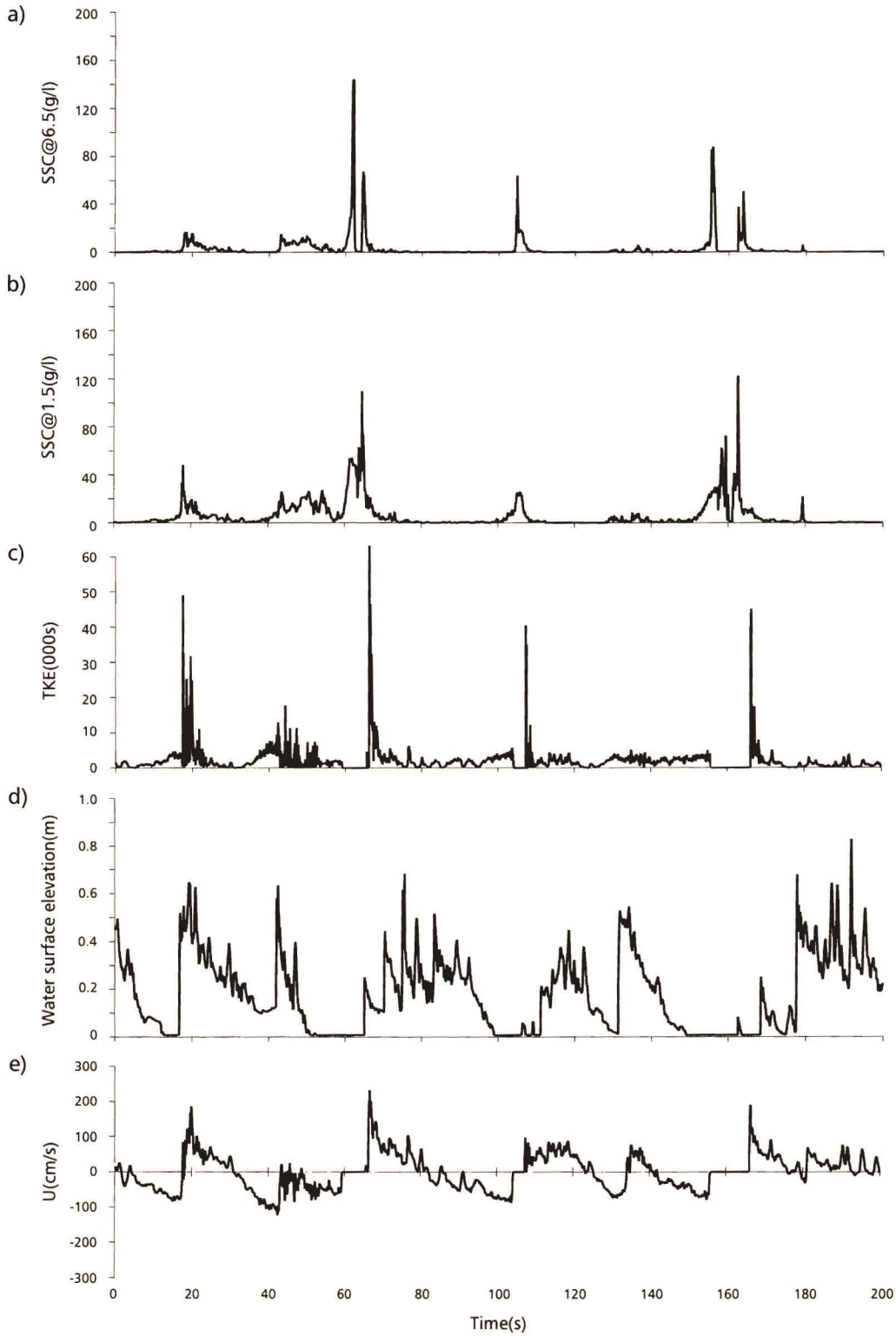

Figure 7. Time series of SSC at 6.5 cm and 1.5 cm elevation (a, b), turbulent kinetic energy (c), water surface elevation (d) and cross-shore velocity (e) from lower swash zone on a falling tide (28-07-1995 11:00).

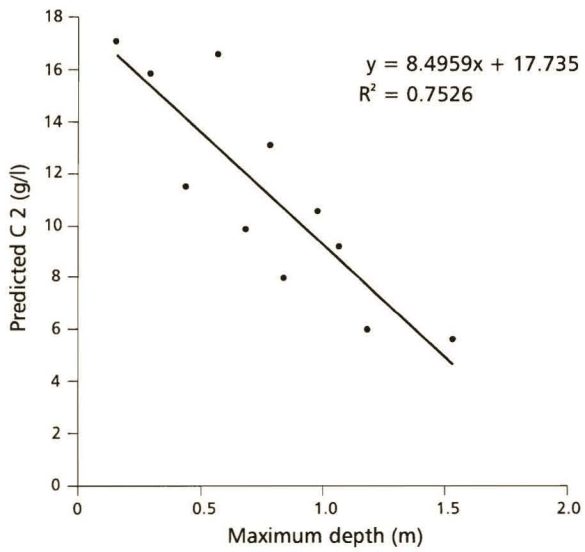

Figure 8. Predicted near-bed SSC at a reference height of 2 cm as a function of maximum water depth during swash events.

is relatively small. It also suggests that the events near the swash fringe generate more suspension than those occurring in deeper water in the surf zone.

JAFFE and SALLENGER (1992) have applied the concept of thresholds in order to examine the frequency distribution of suspension events in time series from the surf zone and we have adopted the same concepts here and applied them to the temporal structure of events within swash/backwash cycles. In this context, a large SSC event is defined here as the event-mean SSC plus three standard deviations while moderate events are defined by the event-mean SSC plus one standard deviation. Results indicate that on average large events occupy only 1–2% of the event, moderate events occur for 9% of the time during a swash zone event, and SSC is lower than the event mean SSC for more than 75% of the event.

The three discrete suspension events in the time series shown in Figure 4 have been ensembled relative to the overall event duration to illustrate the distinctive temporal structure of swash zone events (Figure 9). Corresponding velocities, surface elevations, sediment flux and instantaneous Froude (F_r) numbers are also shown for comparison in Figure 9. SSC reaches a maximum almost immediately after the onset of the uprush phase of the swash. This initial peak is associated with rapidly accelerating flow of a thin sheet of turbulent water flowing up the beach face which corresponds with the onset of high TKE and supercritical flows ($F_r > 1$). The average ramptime (time between the start of SSC increase and maximum SSC) for the uprush phase of the event is 0.6 s (σ = 0.76 s) over 50 swash events. SSC decays after the initial peak to a level between the event mean SSC and 1 event standard deviation above the mean and then decreases more gradually until the end of the uprush phase. The initial decay from peak SSC back to event mean SSC takes 3.6 s ($\pm$ 1.6 s) on average. The majority of sediment which is resuspended during the uprush phase is deposited relatively quickly following the maximum uprush velocity and almost no sand remains in suspension beyond the flow reversal. In contrast, the increase in SSC during the backwash phase is gradual at first and more rapid towards the end of the event as the flow accelerates, thins and becomes supercritical. Average ramptimes between the mean and peak SSC during the backwash were 4.2 s ($\pm$ 3.3 s) while the decay from peak SSC occurred relatively rapidly (0.7 s $\pm$ 0.6 s). The rather complex structure in the SSC event near the end of the backwash cycle is well correlated with fluctuations in the instantaneous Froude number and coincides with the development of turbulent super critical flow conditions. The relatively high SSC which occurs near the end of the backwash phase may have implications for the advection of considerable amounts of sediment into the inner surf zone but may also be important in enhancing the suspended load during uprush events which follow the backwash. An examination of the relative timing of SSC events at each sensor elevation did not indicate any systematic phase shift between the upper and lower elevation as might be expected for a locally generated suspension event. However, due to the rate and intensity of fluid flow under the uprush and backwash and the proximity of the event maxima to the start and end of uprush and backwash phases, it may be necessary to achieve much higher temporal and spatial resolution in swash zone measurements in order to resolve the relative contribution of advection as opposed to locally generated suspension in swash events.

FREQUENCY DEPENDENCE OF CROSS-SHORE SEDIMENT TRANSPORT ON A DYNAMIC FORESHORE

Sediment flux time-series (Figure 10) have been computed from the instantaneous products of cross-shore velocity (u) and SSC shown in Figure 6 which were taken at high tide when sensors were close to being fully immersed. Since the water depth was occasionally less than 15 cm, sensors were intermittently exposed at times during this burst. We have therefore made linear interpolations between points in situations where sensors were not fully immersed. The sediment flux time series indicate that major onshore transport events coincide with accelerating, near peak flow speeds during the start of the uprush cycle and also with maximum SSC. Major offshore transport events coincide with near peak offshore flows, deceleration and maximum SSC near the end of the backwash. The association of high SSC with accelerating and decelerating flows near the start and end of a wave cycle implies that net sediment fluxes may be relatively sensitive to small phase shifts between velocity and SSC.

Figure 11 represents the results of cross-spectral analysis performed on the time-series of SSC and cross-shore velocity taken at high tide when sensors were close to being fully immersed for the duration of the burst in order to examine the relative phase angles and distribution of sediment flux with frequency. The spectra were computed on blocks of 2,048 points with 16–36 degrees of freedom per estimate depending on the local bandwidth. Up to 74% of the variance in the cross-shore velocity occurs in the infragravity band at fre-

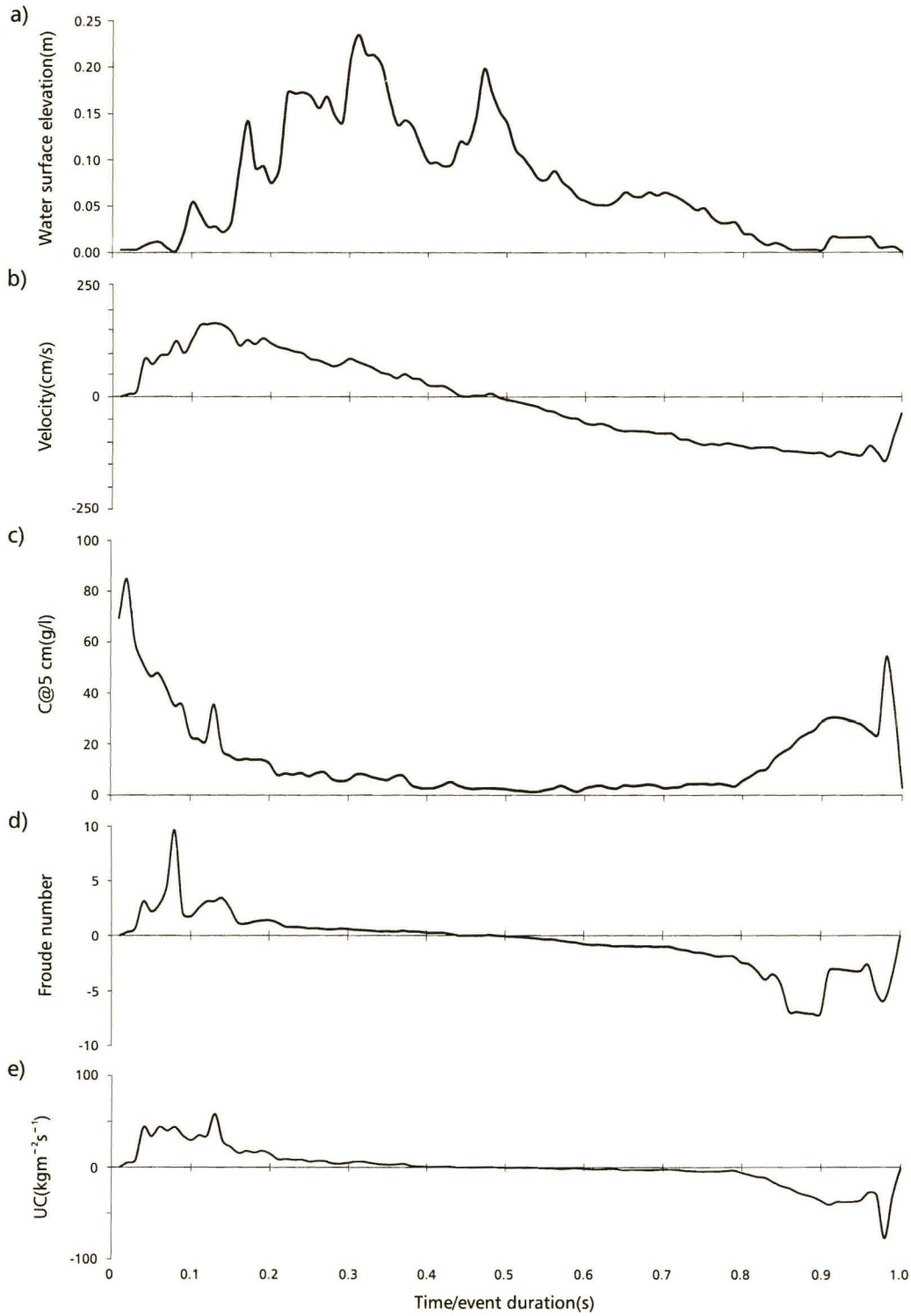

Figure 9. Ensembles of water surface elevation (a), cross-shore velocity (b), SSC at 4.5 cm (c), instantaneous Froude number (d), and cross-product of SSC at 4.5 cm and cross-shore velocity (e) over three swash events. The series have been plotted on a time scale which has been normalised with respect to event duration.

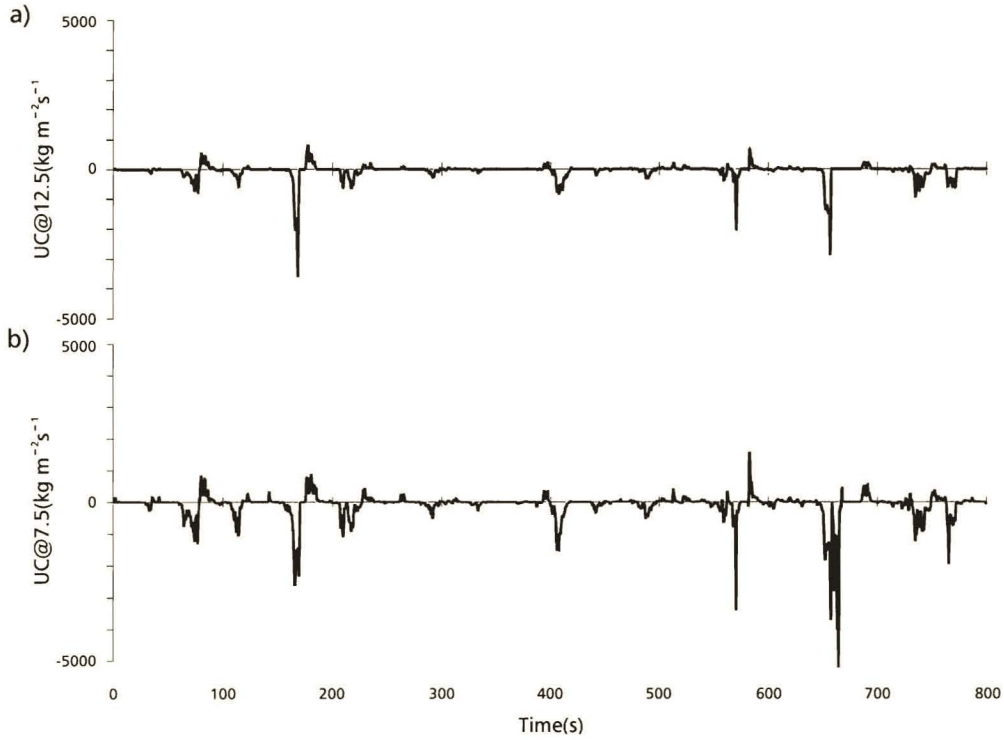

Figure 10. Time series of instantaneous suspended sediment flux at 12.5 cm and 7.5 cm elevation (a, b) from the swash zone/inner surf zone transition (28-07-1995 10:30).

quencies lower than 0.05 Hz while just over 25% of the variance is within the incident band between 0.05 Hz and 1 Hz (Figure 11a). The spectral peak occurs in the infragravity band at 0.033 Hz (~30 s) and completely dominates the spectrum. The SSC spectrum is also dominated by variance at low frequencies (Figure 11b) though this is primarily a result of the intermittent and spiky nature of the SSC time series which tends to "redden" the spectrum. The coherence spectrum (Figure 11c) indicates that the velocity and SSC are coherent over a narrow frequency band in the infragravity range. The cospectrum (Figure 11e) gives the distribution of both the magnitude and direction of fluctuating transport (u'c') with frequency. The fluctuating transport is interpreted as the wave-induced transport which appears to be dependent on the variation of the phase angle between the SSC and the instantaneous wave-induced velocity with frequency. The phase spectrum (Figure 11d) indicates that peak SSC leads the peak velocities by just under 90° in the infragravity band. This lends support to the interpretation that onshore transport occurs largely during the early phases of uprush before the peak velocity is reached. Conversely major offshore transport events are associated with phases just before the zero upcrossing.

Beach profiles measured at low tide and after the process measurements at high tide did not differ significantly indicating that the foreshore was in stable equilibrium over the half tidal cycle (Figure 2). On the other hand depth of activity measurements (Figure 12) indicated that short term fluctuations in bed level occurred over much shorter time scales in response to the large instantaneous fluxes associated with the cross-shore infragravity motions. The measurements analysed here suggest that foreshore equilibrium may be brought about by relatively small differences in the velocity—SSC phase relationship.

DISCUSSION AND CONCLUSIONS

Suspension events in the swash zone are characterised by a distinctive temporal structure. High concentrations seem to be associated with high bed shear stresses and turbulence (TKE) generated by the rapidly accelerating flows at both the start and end of the uprush and backwash. The high concentrations towards the end of backwash cycles in particular, appear to coincide with the development of supercritical flow conditions (instantaneous Froude number > 1), high TKE and the occurrence of backwash ripples. In uni-directional flows over non-cohesive sand beds, sustained supercritical flows lead to an unstable bed and the development of bedwaves or anti-dunes (SIMONS and RICHARDSON, 1961). Anti-dune bedforms or backwash ripples (BROOME and KOMAR, 1979) tend to form on low gradient dissipative beaches when an undular hydraulic jump develops through collision of supercritical backwash with an incoming swash bore. This generates undulations in the backwash itself which then result in the bedwaves. Supercritical flow conditions, hydraulic jumps and backwash ripples were often visible on the beach

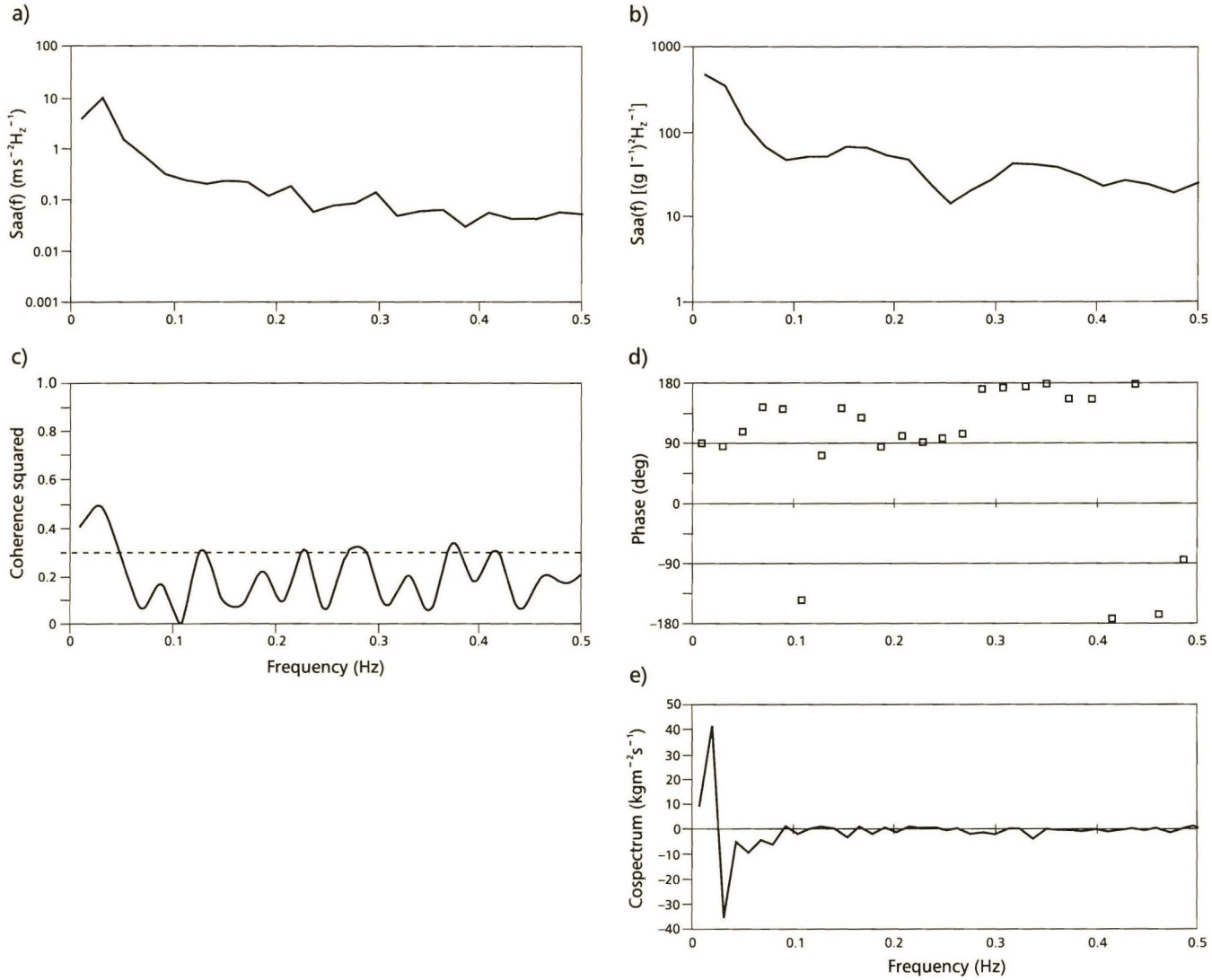

Figure 11. Cross spectral analysis of SSC and cross-shore velocity at high tide (28-07-1995 10:30) including autospectra of velocity and SSC (a, b), coherence and phase spectra (c, d) and the cospectrum (e). Note: spectra were computed on blocks of 2,048 points with between 16–36 degrees of freedom per estimate depending on the local bandwidth; the 95% confidence limit for zero coherence is shown in c.

face during the waning stages of backwash events, these roughness features undoubtedly contribute to the enhancement of SSC during the latter portion of many swash events and may account for the distinctive secondary peaks in SSC which characterise the end of many backwash suspension events. These bedforms are generally wiped out during the intense short duration acceleration and peak uprush phase of the next swash event; the remainder of the uprush event is characterised by a steady deceleration and declining flow regime. Therefore it seems likely that high concentrations during the uprush phase are controlled more by intense turbulence and high stresses associated with the front of shoreward propagating swash bores than by the development of bedforms associated with super-critical flows. However, high SSC close to the end of the backwash may lead to considerable advection of SSC into the inner surf zone and also to enhanced SSC during subsequent uprush events. It is also possible that velocity asymmetry induced by percolation and ground-water resurgence may also lead to transport asymmetry and enhanced SSC on the backwash. Further measurements with greater spatial and temporal resolution may be required to resolve the relative contributions of advection, diffusion and convection and the effects of percolation and resurgence to swash zone suspension events.

A number of contemporary physically based models for sediment transport in the nearshore are based on the assumption of a direct dependence between SSC, sediment transport rates and the instantaneous bed shear stresses based on local fluid velocity field (*e.g.* BAGNOLD, 1966; BAILARD, 1981). In the swash zone, major suspension and transport events co-

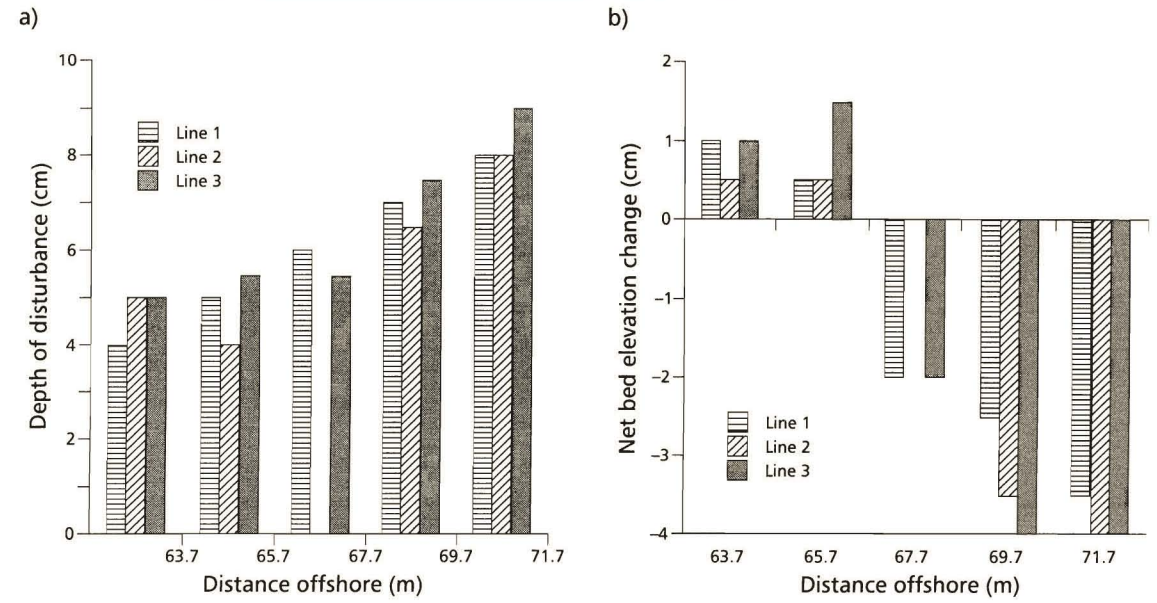

Figure 12. Patterns of short term (2–3 infragravity swash events) depth of sediment reactivation (a) and net bed elevation changes (b) on the mid foreshore.

incide closely with maximum TKE levels derived from local 3-D velocity measurements implying that a velocity based transport model should perform reasonably well in the high energy infragravity swash environment. However, it is clear that the net transport will be a small difference between two large quantities and therefore prediction is likely to be complicated by relatively small differences in the phase angle between velocity and SSC and also by the presence or absence of bedforms which may develop during the backwash cycle leading to enhanced SSC levels.

ACKNOWLEDGEMENTS

The authors gratefully acknowledge funding from the University of Auckland Research Committee in support of this research. Thanks also to Dr. Kevin Parnell, Shane Thomson, Murray Bansall-Allen, Janine Pritchard, Libby Boak, and Alex Lee for their assistance while in the field. The authors are grateful for comments provided by Troels Aagaard and an anonymous reviewer which lead to significant improvements of the final manuscript.

LITERATURE CITED

AAGAARD, T. and GREENWOOD, B., 1994. Suspended sediment transport and the role of infragravity waves in a barred surf zone. *Marine Geology,* 118, 23–48.

BAGNOLD, R.A., 1966. An approach to the sediment transport problem from general physics. *U.S. Geological Survey Professional Paper No. 422-I.*

BAILARD, J.A., 1981. An energetics total load sediment transport model for a plane sloping beach. *Journal Geophysical Research,* 86, 10938–10954.

BEACH, R.A. and STERNBERG, R.W., 1992. Suspended sediment transport in the surf zone: response to incident wave and longshore current interaction. *Marine Geology,* 108, 275–294.

BEACH, R.A. and STERNBERG, R.W., 1991. Infragravity driven suspended sediment transport in the swash, inner and outer surf zone. *Proceedings Coastal Sediments '91.* New York; ASCE, pp. 114–128.

BROOME, R. and KOMAR, P.D., 1979. Undular hydraulic jumps and the formation of backwash ripples on beaches. *Sedimentology,* 26, 543–559.

DICK, J.E.; ERDMAN, M.R., and HANES, D.M., 1994. Suspended sand concentrations due to shoaled waves over a flat bed. *Marine Geology,* 119, 67–73.

DYER, K.R., 1986. *Coastal and Estuarine Sediment Dynamics.* London; Wiley, 342p.

HANES, D., 1991. The structure of events of intermittent suspension of sand due to shoaling waves. *In:* LEMEHAUTE B. and HANES D.M., (eds), *The Sea, Ocean Engineering Science.* New York: Wiley, pp. 941–951.

HAYWARD, B.W., 1983. Geological map of New Zealand: Sheet Q11 Waitakere (1:50000). Map 1 (1 Sheet) and notes (29 p). New Zealand Department of Scientific Research.

HESSELL, J.W.D., 1988. The climate and weather of Auckland. *New Zealand Meteorological Society Publication,* 115(19).

HORN, D.P. and MASON, T., 1994. Swash zone sediment transport modes. *Marine Geology,* 120, 309–325.

JAFFE, B. and SALLENGER, A., 1992. The contribution of suspension events to sediment transport in the surf zone. *Proceedings International Conference Coastal Engineering* (ASCE), pp. 2680–2693.

LOHRMANN, A.; CABRERA, R., and KRAUS, N.C., 1994. Acoustic Doppler Velocimeter (ADV) for laboratory use. *Proceedings Symposium on Fundamental and Advancements in Hydraulic Measurements and Experimentation.* New York: ASCE, pp. 351–365.

NEILSEN, P., 1984. Field measurements of time-averaged suspended sediment concentrations under waves. *Coastal Engineering,* 8, 51–72.

OSBORNE, P.D.; VINCENT, C.E., and GREENWOOD, B., 1994. Measurement of suspended sand concentrations in the nearshore: field intercomparison of optical and acoustic backscatter sensors. *Continental Shelf Research.* 14(2/3), 159–174.

SIMONS, D.B. and RICHARDSON, E.V., 1961. Forms of bed roughness in alluvial channels. *Journal Hydraulic Division American Society Civil Engineers,* 87(3), 87–105.